A smoothed interface interaction method for compressible flow

X. Y. Hu[1], B. C. Khoo[2] and N. A. Adams[1]

[1] *Lehrstuhl für Aerodynamik, Technische Universität München 85747 Garching, Germany*
[2] *Department of Mechanical Engineering, National University of Singapore, 119260 Singapore*

Abstract. While the interface interaction method (I-GFM) [5] can handle multi-fluid and complex moving boundary problems effectively, it approximates the interface at cell wall and losses some accuracy associated with the sub-grid interface defined by the level set. In this paper, a smoothed interface is obtained by including information of the sub-grid interface implicitly. Numerical results suggest greater accuracy and less conservation error on the interface or boundary are obtained with negligible increase in computational cost.

1 Introduction

Two main Eulerian numerical approaches, front tracking and front capturing, have been developed for compressible flows with interface. The level set technique enables a combination of these two approaches [9]. The ghost fluid method (GFM) [3] offers a fairly simple way to implement in multi-dimension and enables multi-level time integration other than dimensional time splitting. In our previous work [5], the interface interaction method (I-GFM) was proposed to obtain the ghost fluid states according to the interface interaction.

The I-GFM is able to handle multi-fluid problems with large difference of states and material properties at interface while still keeping to the simplicity of the original GFM. However, it approximates the interface at cell wall and losses accuracy associated with the sub-grid interface defined by the level set function. This approximated interface is not smooth either because the connected cell walls possess the shape of "stair steps". In this paper, a smoothed interface is obtained by modifying the values on nodes nearest to the interface according to the volume fractions of real and ghost fluids. The current method is based on the standard level set technique and simple to implement.

2 Modification to the I-GFM scheme

In the I-GFM, a real fluid is only defined on the nodes (real nodes) with real states on one side of the interface . On the other side of the interface, the corresponding ghost fluid is defined on the nodes (ghost nodes) with ghost states inside the narrow band of the interface. No fluid is defined on the rest of nodes (empty nodes) with any state (see Fig.1 where fluid 1 and fluid 2 are separated by the interface). Specifically, the ghost states are obtained by the following procedures. First, the ghost nodes are filled with reference states, including pressure, velocity and entropy (for isobaric fix [3]), which are extended from the real states of the same fluid along the interface normal direction. Second, the interface interaction is solved on the ghost node using the (initial) reference state and the real state of the second fluid along the interface normal direction to obtain the interface

state; then the (initial) reference state is replaced by the interface state and taken to be the 'final' ghost state.

When the two fluids are solved with an one-phase solver separately, both the real states and ghost states are utilized as cell-averaged values and taken to fully occupy the associated cells. This is true for the nodes sufficiently far from the interface. However, for the nodes nearest to the interface, since the cells are cut by the interface, the states on such nodes are strictly no longer cell-averaged values (see Fig. 1). Therefore, for a such ghost node there is a portion of real fluid in the cell and so forth for a such real node. If the states on these nodes are approximated as cell-averaged values, it implies that the equivalent approximated interface coincides with the cell walls. It is not accurate because the sub-grid interface location as indicated by the level set function is lost. As shown in Fig.1, the approximated interface is not smooth either because the connected cell walls have shape like that of "stair steps". Since this interface can only shift its location between nearby cell walls other than move smoothly, it may lead to a potential difficult if the proposed interface moves slowly or oscillates with an amplitude smaller than the grid size. In addition, as shown later, when the I-GFM is applied to complex moving boundary problems, the boundary of such connected cell walls is equivalent to a rough surface which may produce noisy or oscillating flow field [2].

In this paper, both the real fluid and ghost fluid are defined on the nodes nearest to the interface according to their volume fractions, c_{rl} and c_{gh}, $c_{rl}+_{gh} = 1$, of the associated cell. Therefore, reference state extension is no longer necessary for such ghost nodes, and the interface interaction is solved directly with the real states of the two fluids. After the interface state is obtained, the associated conservative variables are averaged based on volume fractions, that is

$$W_{gh}(p, \rho, \mathbf{v}) = c_{rl} W_{rl}(p, \rho, \mathbf{v}) + c_{gh} W_I(p, \rho, \mathbf{v}). \tag{1}$$

This is equivalent to obtain a smooth interface by including information of the sub-grid interface location implicitly. The above modification is implemented in a node-by-node

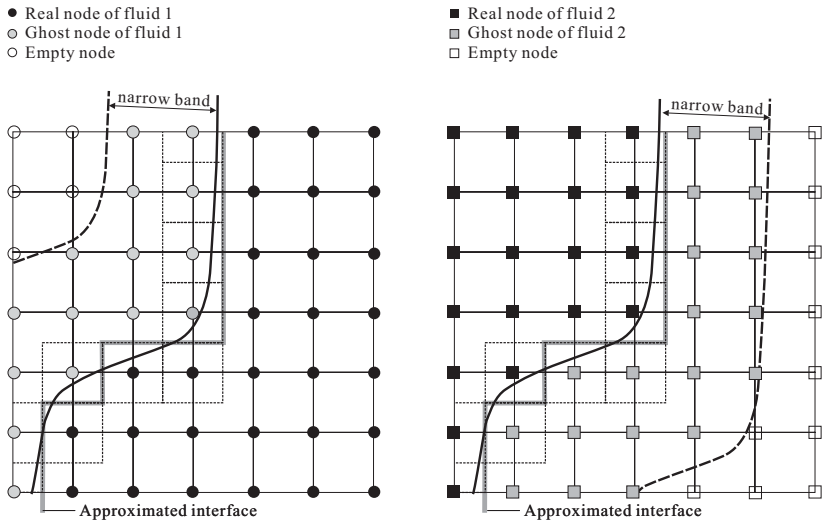

Fig. 1. Schematic for fluids, nodes, states and interface

fashion and only on the nearest nodes to the interface, hence, there is only negligible increase in computation cost.

With the standard level set technique, the volume fractions for fluids 1 and 2 can be approximated by

$$c_{rl}^1 = c_{gh}^2 = H(\phi, \varepsilon), \quad c_{gh}^1 = c_{rl}^2 = 1 - H(\phi, \varepsilon) \tag{2}$$

where $H(\phi, \varepsilon)$ is the smoothed Heaviside function and ε is a small positive number, such as the spatial step. A possible way to calculate $H(\phi, \varepsilon)$ is contouring based on the node level set value. Consider a two-dimensional level set function, defined on a Cartisian grid with $\Delta x = \Delta y = \varepsilon$, the schematic for contouring is shown in Fig 2. The level set on a node O has a value of ϕ and a normal direction with angle α to the x direction. In the associated cell $ABCD$, the zero level set can be approximated with the straight line segment EF. If the area $s(\phi)$ occupied by the real fluid is calculated, the volume fraction is normalized to

$$c_{rl} = \frac{s(\phi)}{\varepsilon^2} = H(\phi, \varepsilon). \tag{3}$$

As shown in in Fig. 2, two cases, i.e. $\phi > 0$ and $\phi < 0$, need to be considered. The relation between the two cases is $s^+ = \varepsilon^2 - s^-$, in which s^+ is $s(\phi)$ for $\phi > 0$ and s^- is $s(\phi)$ for $\phi < 0$. It is easy to find that s^+ is the combination of a half cell and the area enclosed by the polygon $RBEFS$, which is the difference of the parallelogram $RGFS$ and ΔBGE. As such, s^+ is obtained as

$$s^+ = \begin{cases} \frac{1}{2}\varepsilon^2 + D\phi & \text{if } \Lambda < 0 \\ 0 & \text{if } \Lambda > \Gamma \\ \frac{1}{2}\varepsilon^2 + D\phi - \frac{1}{2}\frac{\varepsilon\Lambda^2}{\Gamma} & \text{else} \end{cases}. \tag{4}$$

where $D = L_{RS} = \varepsilon \min(\frac{1}{|cos\alpha|}, \frac{1}{|sin\alpha|})$, $\Gamma = 2L_{A'R} = \sqrt{D^2 - \varepsilon^2}$ and $\Lambda = L_{BG} = \frac{\Gamma}{2} + \frac{D|\phi|}{\varepsilon} - \frac{\varepsilon}{2}$. Accordingly, it can be further shown that

$$H(\phi, \varepsilon) = \begin{cases} 0 & \text{if } \Lambda > \Gamma, \quad \phi < 0 \\ \frac{1}{2} + \frac{1}{\varepsilon^2}D\phi + \frac{1}{2}\frac{\Lambda^2}{\varepsilon\Gamma} & \text{if } \Gamma \geq \Lambda \geq 0, \quad \phi < 0 \\ \frac{1}{2} + \frac{1}{\varepsilon^2}D\phi & \text{if } \Lambda < 0 \\ \frac{1}{2} + \frac{1}{\varepsilon^2}D\phi - \frac{1}{2}\frac{\Lambda^2}{\varepsilon\Gamma} & \text{if } \Gamma \geq \Lambda \geq 0, \quad \phi > 0 \\ 1 & \text{if } \Lambda > \Gamma, \quad \phi > 0 \end{cases}. \tag{5}$$

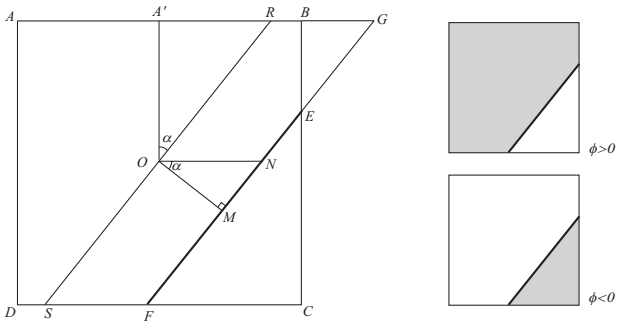

Fig. 2. Schematic for level set contouring

Since the I-GFM can be directly applied to complex moving boundary problems by simply switch off the second fluid and update the level set with prescribed or inertia-coupled velocity, the above mentioned modification can be applied fairly straightforward. Note that, since the solid wall boundary condition is used, the reference state extension may be replaced with the mirroring technique [1]. On comparing to [4], the present method is simpler because no dimensional time splitting is necessary and the level set technique is employed for the complex boundary description as well as boundary condition treatment.

3 Numerical examples

For all the test cases, the one-phase calculations are carried with the 5th order WENO-LF [7] and 3rd order TVD Runge-Kutta [11]. Before each sub-time-step of TVD-Runge-Kutta, the interface condition is solved once. In the one-dimensional examples, unless otherwise stated, the number of grid points is 200 and the referenced exact solution is sampled on 200 grid points too. All runs are carried out with the CFL of 0.6.

Multi-fluid Sod's problem We consider an air-helium shock tube problem with the following initial data:

$$(\rho, u, p, \gamma) = \begin{cases} (1, 0, 1, 1.4) & \text{if } x < 0.5 \\ (0.125, 0, 0.1, 1.667) & \text{if } x > 0.5 \end{cases}. \tag{6}$$

This case is computed to time $t = 0.15$. The relative mass variations for the left medium and right medium during the computation can be calculated by

$$\Delta m^n = \frac{\sum_{j=0}^{j=K^n} \rho_j^n + c_{rl,I}^n \rho_I^n}{\sum_{j=0}^{j=K^0} \rho_j^0 + c_{rl,I}^0 \rho_I^0}, \tag{7}$$

where ρ_j is the cell-averaged density on node j, ρ_I is the corresponding quantity of a cell with cutting interface, the superscript o and n are for the initial condition and the nth time step values, respectively, and K is the number of cells fully occupied by the left or right medium. In a similar way, the total mass variations can also be obtained.

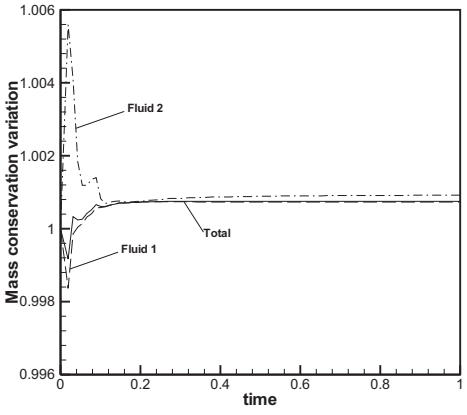

Fig. 3. Mass variations for the multi-fluid sod problem

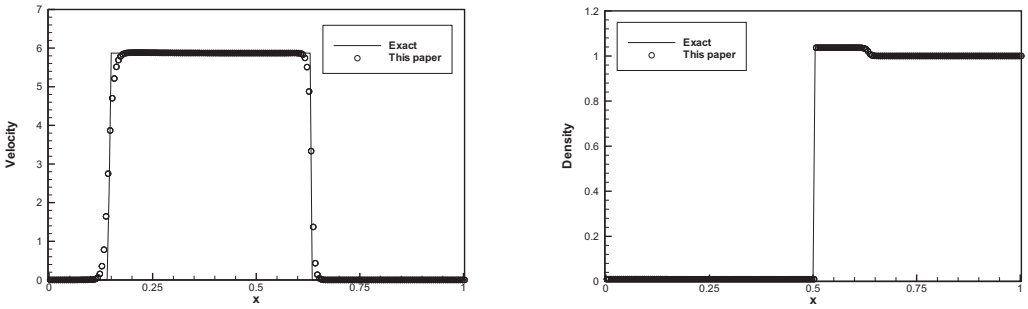

Fig. 4. Underwater explosion problem

Figure 3 presents the relative conservation variations of the left medium mass, the right medium mass and the total mass. On comparing to the results in I-GFM (Fig. 14 of [5]), the current method produces only about 50% and 25% of mass conservation errors for the two separated fluids respectively and about the same total mass conservation error.

Underwater explosion problem A real gas equation of state is used for the explosive and Tait's equation of state for the water medium. The initial conditions are given as

$$(\rho, u, p, \gamma) = \begin{cases} (0.01, 0, 1000, 2) & \text{if } x < 0.5 \\ (1, 0, 1, 7.15) & \text{if } x > 0.5 \end{cases}. \tag{8}$$

In this underwater explosion, the high pressure explosive products bubble expands very slowly comparing to the transmitted or reflected wave front speed. Figures 4 shows the computed results at time $t = 0.0008$. Note the current results present a more accurate solution for the rarefaction wave and the transmitted shock wave than that of the I-GFM; the latter depicts a slight overshot at the rarefaction wave and small difference of velocity at the water-explosive interface (see Fig. 12 in [5]).

Moving wall problem We consider a gas confined between two reflectiong walls at $x_l = 0.5 + u_l t$ and $x_r = 1.0$ with constant $u_l = -0.5$. The initial conditions are

$$[\rho(x), u(x), p(x)] = \left[1 + 0.2\cos(2\pi x - \pi), 2u_l(1-x), \rho(x)^{1.4}\right] \tag{9}$$

in which the entropy $s(x) = 1$. We calculate this case to time $t = 0.5$. Since the analytic solution is smooth, the entropy stays constant. The boundary and total entropy error is calculated by

$$err_{bry} = |s_{bry} - 1|, \quad err_{ttl} = \frac{\sum_{j=0}^{j=K^n} |s_j^n - 1| + c_{rl,bry}^n |s_I^n - 1|}{K^0 + c_{rl,bry}^0}. \tag{10}$$

Table 1. Errors in moving wall problem

$1/h$	Δm	err_{tot}	err_{bry}
200	7.0×10^{-4}	7.5×10^{-7}	4.6×10^{-5}
400	3.5×10^{-4}	1.4×10^{-7}	1.1×10^{-5}
800	1.8×10^{-4}	2.5×10^{-8}	2.1×10^{-6}

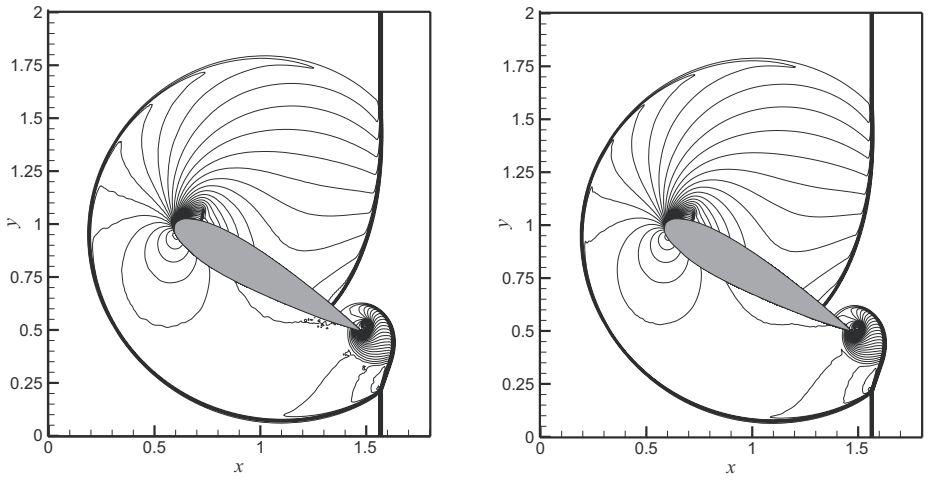

Fig. 5. Shock diffraction on airfoil: calculated pressure contours with I-GFM (left) and the current method (right) on 360×400 grid, $t = 1.04$

The results for err_{bry}, err_{ttl} and Δm in Table 1 show that the current moving boundary treatment is second-order accurate and has first-order convergence rate for the mass conservation error, which suggest the same order of accuracy and convergence rates as the method in [4].

Shock diffraction on airfoil We consider Mach 1.5 shock diffraction past a NACA0018 airfoil with $+30^o$ angle of attack [8]. The level set is built from a polyline consisting 200 control points [6]. Figure 5 shows the computed results using I-GFM and the current method at time $t = 1.04$. It is found that the current method produces sharper diffraction shock front and has no noise compared to the results with the I-GFM which is attributed to the approximated non-smooth boundary. It is noted too, on comparing to the results in [10] on a 500×500 grid with immersed boundary method, both the I-GFM and the present method suggest higher order accuracy by which sharper shock wave front and refined flow structures near the airfoil head and tip are produced.

References

1. R. Arienti, P. Hung, E. Morano, J. E. Shepherd: J. Comput. Phys. **185**, 213 (2003)
2. G. Ben-Dor: Shock wave reflection phenomena. Springer, Newyork, 1992
3. R. Fedkiw, T. Aslam, B. Merriman, S. Osher: J. Comput. Phys. **152** 457 (1999)
4. H. Forrer, M. Berger: Flow simulation on Cartisian grids invloving complex moving geometries flows. In: *Int. Ser. Numer. Math., 129, Birkhäuser, Basel, 1998*
5. X. Y. Hu, B. C. Khoo: J. Comput. Phys. **198**, 35 (2004)
6. X. Y. Hu, B. C. Khoo: Numerical studies on shock cell interaction. In: *The 25th International Symposium on Shock Waves , Beijing, July 20 - 25, China, 2004*
7. G. S. Jiang, C. W. Shu: J. Comput. Phys. **126** 202(1996)
8. M. Mandella, D. Bershader: *AIAA paper No. 87-0328*
9. S. Osher, J. A. Sethain: J. Comput. Phys. **79** 12 (1988)
10. R. C. Ripley, D. R. Whitehouse, F. S. Lien: Effect of mesh topology on shock wave loading computations. In: *CFD2003, Vancouver, May 28-30, Cananda, 2003*
11. C. W. Shu, S. Osher: J. Comput. Phys. **77** 439 (1988)